Mass Comparisons and Investigations into the Volatile and Semivolatile Fraction of Particles

7. Comparison of Two Methods for Obtaining Quantitative Mass Concentrations from Aerosol Time-of-Flight Mass Spectrometry Measurements

i. Introduction

Over the past two decades, the number of studies on airborne particulate matter has increased substantially due to increased awareness of the role of aerosols in reducing visibility, affecting climate change, and endangering human health (141,143,234-238). Health risks have been shown for particles with aerodynamic diameters less than 2.5 μm ($PM_{2.5}$), based on mortality rates which show a positive correlation with particles in this size range (239). Therefore, it is very important to perform regional-scale long term monitoring in order to better understand the major sources impacting the annual $PM_{2.5}$ mass concentrations.

Although traditional off-line filter based measurements are able to provide robust information on aerosol mass concentration and chemical composition, they still have limitations such as low time resolution, sampling artifacts (240), and very limited information on aerosol mixing state which is essential for understanding the impacts of aerosols on climate and visibility (241). Real-time single particle mass spectrometry (SPMS) measurements provide continuous on-line information on single particle size and chemical composition (242-244). These measurements can be used to provide further insight into the associations between chemical species within individual particles, allowing one to link composition with specific sources and atmospheric processing. Particles are rapidly analyzed (<1 ms), minimizing the changes in particle morphology and the repartitioning of chemical species during the analysis. Despite these advantages, it has been a challenge for real-time SPMS instruments to provide quantitative information on aerosol mass concentrations. Several factors present obstacles in quantifying SPMS measurements. First, particle transmission efficiency is size-dependent and needs to be corrected using number concentrations from other co-located instruments (173). Second, in most real-time SPMS methods, the ion signals in the mass spectra for identical particles can vary considerably from shot-to-shot due to inhomogeneities in the laser beam (245). Third, instrument sensitivities to different aerosol chemical species vary (161,246), and can change as a function of matrix composition (247) and particle size (85). Fourth, when instrument operation and data acquisition are controlled by the same computer, the ability to detect incoming particles decreases with increasing ambient particle concentration due to instrument busy time (248).

Due to the aforementioned issues, the quantitative potential of SPMS measurements has not been fully realized. A number of efforts have been dedicated to acquiring high temporal resolution quantitative information from SPMS data by scaling with co-located reference measurements (30,36,85,248-251). Among the various SPMS instruments developed to date, most of the quantification efforts have been applied to

aerosol time-of-flight mass spectrometry (ATOFMS), which acquires real-time information on single particle aerodynamic diameter (D_a) and chemical composition. Although ATOFMS measures D_a, only Allen et al. (248,249), Bhave et al. (85), and Moffet et al. (251) used D_a-based reference measurements to reconstruct quantitative results from ATOFMS data. Allen et al. (248,249) and Bhave et al. (85) used a micro-orifice uniform deposit impactor (MOUDI) as the reference method for quantification. Typical MOUDI measurements have a time resolution of 5 ~ 8 hours and a size resolution of 4 bins per decade. Moffet et al. (251) compared ATOFMS measurements against aerodynamic particle sizer (APS) measurements, which provide higher time and size resolution than the MOUDI, to obtain quantitative number concentrations.

In this paper, we compare both MOUDI scaling and APS scaling methods to quantify ATOFMS single particle measurements taken during a field campaign conducted in central California. We adapt the busy-time estimation methodology of Allen et al. (248) to account for recent changes in the ATOFMS data acquisition procedure. We advance the APS scaling methodology of Moffet et al. (251) by utilizing composition dependent density values to obtain quantitative mass concentrations. We present the first evaluation of scaled ATOFMS mass concentrations against multiple, independent co-located $PM_{2.5}$ measurement devices. These scaling approaches will be used for future ambient studies to obtain quantitative ATOFMS mass concentrations and can be easily applied to other SPMS measurements.

ii. Experimental

As part of the California Regional Particulate Air Quality Study (CRPAQS), two ATOFMS instruments were operated continuously, sampling ambient aerosols from November 30, 2000 to February 4, 2001. The two sampling sites were an urban site in Fresno and a rural site in Angiola, both of which are located in central California (252). Single particle size and chemical composition information on more than 2 million particles was acquired at each site. ATOFMS data are scaled with MOUDI (MSP Corp.) measurements at Fresno and with APS (TSI 3320) measurements at Angiola to obtain quantitative information. Other $PM_{2.5}$ measurements are also used for comparison and evaluation, including a beta attenuation monitor (BAM, Met One BAM 1020), tapered element oscillating microbalance (TEOM, Rupprecht & Patashnick TEOM 1400A), dust aerosol monitor (TSI DustTrak 8520), nephelometer (Radiance Research M903), and aethalometer (Magee Scientific RTAA1000). Only the measurements taken from January 9, 2001 to February 4, 2001 are presented in this work, representing 711,289 particles in Fresno and 614,915 particles in Angiola.

a. ATOFMS Data Acquisition

ATOFMS acquires single particle diameter utilizing particle time-of-flight and obtains particle chemical composition based on the mass spectra. The design and operating principles of ATOFMS have been described in section 1.5.1 and are also discussed in detail elsewhere (127). Not all particles that are sized produce a corresponding mass spectrum, due to differences in the particle trajectories between the light scattering and ion source regions. Particles that produce both aerodynamic diameters and mass spectra are called hit particles, whereas particles that only yield aerodynamic diameters are called missed particles. A special ATOFMS operating

condition is the fast scatter mode. When operating under this condition, ATOFMS only records missed particle size information without attempting to acquire mass spectra. Fast scatter measurements were often used for obtaining overall particle size distribution.

After the field study, an in-house software program was used to calibrate the mass spectra and make a list of the individual ion peaks for each particle. These peak lists were then imported into a single particle mass spectrometry data analysis tool YAADA, for further analysis (160).

b. MOUDI Measurements

The MOUDI is based on particle impaction and has been extensively used for obtaining size resolved particle mass and composition measurements (253). During the CRPAQS study, MOUDI data were collected at Fresno during six intensive operating periods (IOPs) within the time of interest for this study: 31 January 1000-1600; 1 February 0500-1000; 2 February 0000-0500; 2 February 1000-1600; 3 February 0500-1000; and 3 February 1600-2400. Angiola MOUDI measurements were not used in this study since we were unable to accurately estimate ATOFMS busy time at that site due to a change in the data acquisition hardware in the middle of the study period.

c. APS Measurements

The APS provides information on both single particle number concentrations and aerodynamic diameter via light scattering and time-of-flight measurements (254). It detects particles in the size range of 0.3 μm to 20 μm, with accurate size-resolved counting of particles with aerodynamic diameters between 0.5 and 20 μm. APS measurements were not collected at Fresno during the CRPAQS. At Angiola, measurements were obtained with a commercial APS (TSI 3320, Minnesota) from December 1, 2000 to February 4, 2001 with a temporal resolution of 5 minutes. The APS data were averaged over 1-hour time periods. These hourly data are used in the scaling procedure described below

iii. Results and Discussion

a. Scaling with MOUDI

Previous investigations have shown that by comparing co-located ATOFMS and MOUDI data, quantitative information on particle mass concentrations can be acquired from ATOFMS measurements (248,249). The advantage of scaling with MOUDI measurements is that they not only provide information on size segregated total particle mass concentrations, but also the size segregated concentrations of individual chemical species which allow the derivation of ATOFMS relative sensitivity factors to different chemical species (85). The disadvantage is that MOUDI samples are analyzed offline and provide coarse temporal- and size-resolution data. In this work, we adapt and modify the busy time estimation method developed by Allen et al. (248) and use it to scale the Fresno ATOFMS dataset with MOUDI measurements.

1. ATOFMS Busy Time

Busy time (t_b) is defined as the amount of time that an ATOFMS instrument cannot detect incoming particles because it is busy processing data from a particle that just arrived. Previous studies revealed that three parameters are needed to compute ATOFMS instrument busy time: the time required to record a missed particle (*A*), the time required to record the first hit particle in a folder (*B*), and the incremental increase in time required to save each subsequent hit particle in a folder (*C*). Laboratory experiments have been conducted to estimate these parameters, but when lab-based parameters are applied to field data, the results are at times not physically meaningful (e.g., busy time occasionally exceeds total sampling time). Thus, empirical methods have been developed to estimate busy time directly from field data. During the 1999 Bakersfield Instrument Intercomparison Study (BIIS), the ATOFMS instrument was operated alternately in normal data collection mode and fast scatter mode. Allen et al. (248) used data collected in fast scatter mode to estimate particle arrival rates (λ). They demonstrated that Poisson with Busy Time (PBT) distributions in conjunction with λ values can be used to compute *A*, and that this information in combination with the particle data collected in normal operating mode can be used to compute *B* and *C*.

During CRPAQS and subsequent field campaigns, ATOFMS instruments were not routinely operated in fast scatter mode so the methodology of Allen et al. (248) cannot be applied directly. In the present study, we adapt the previous methodology to estimate busy time parameters for the ATOFMS instrument that was stationed at Fresno. An analysis of the Fresno data set reveals five discrete time periods when the rate of missed particle detection (r_m) doubled while the hit particle detection rate (r_h) dropped substantially: 16 January 2150 – 17 January 0200; 28 January 0335 – 1115; 31 January 0430 – 0845; 1 February 0750 – 1040; and 2 February 0610 – 1000. As an example, **Figure 54** illustrates the time series of r_m and r_h in 6-minute intervals throughout 28 January. Several possible reasons for these "high-miss periods" were explored, but a definitive conclusion was not obtained. Nevertheless, even without a full understanding, it was determined that the data from these high-miss periods may be exploited to calculate *A*. The strong anti-correlations between r_m and r_h suggest that the busy time associated with missed particles caused the hit rate to drop during each high-miss period. Assuming that the degree to which r_h drops during the high-miss periods is determined by the time remaining to record hit particles after all missed particles are recorded,

$$\frac{N_{Hit}}{N_{EstHit}} = \frac{t - (A \cdot N_{Missed})}{t - (A \cdot N_{EstMissed})} \tag{5.1}$$

where *t* is the length of each sampling interval; N_{Hit} and N_{Missed} are the number of hit and missed particles recorded during a sampling interval; and N_{EstHit} and $N_{EstMissed}$ are the estimated number of hit and missed particles if the high-miss event had not occurred. As illustrated in **Figure 54a**, N_{EstHit} and $N_{EstMissed}$ are calculated in 6-minute intervals by linear interpolation of r_h and r_m, respectively, over each high-miss period. By solving

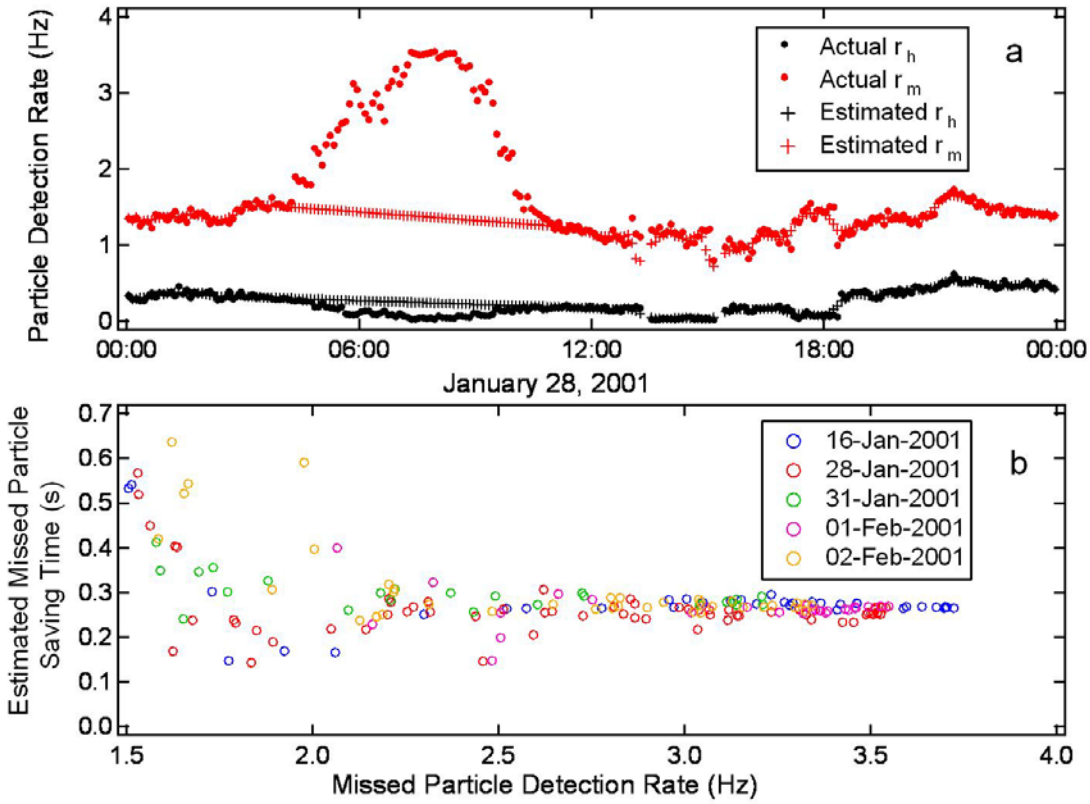

Figure 54: (a) Linear interpolation over the Fresno high-miss period to obtain estimated hit counts and estimated missed counts for the period of January 28th, 3:35 – 11:15; (b) estimated missed particle recording time vs. missed particle detection rate for all five high-miss periods with a time resolution of 6 minutes for Fresno dataset.

Equation (5.1) for A, we obtain:

$$A = \frac{t \cdot \left(N_{Hit} - N_{EstHit}\right)}{(N_{Hit} \cdot N_{EstMissed}) - (N_{EstHit} \cdot N_{Missed})} \tag{5.2}$$

The values of A calculated during 6-minute time intervals within each high-miss period are plotted against r_m in **Figure 54b**. The five different colors in **Figure 54b** represent results from different high-miss periods. As can be seen, there is remarkable consistency in the values of A across all five high-miss periods when r_m exceeds 2.5 Hz. These time intervals occurred at the peak of each high-miss period, when the instrument was devoting the vast majority of the sampling time to detecting missed particles. Thus, the A values calculated during these times are most robust. Whether setting the minimum r_m thresholds at 2.0, 2.5, 3.0, or 3.5 Hz, the mean value of A remains fairly constant at 0.26 seconds with the standard deviation being less than 0.05 seconds. Based on the above inspection, we use 3.0 Hz as the minimum r_m threshold since at this frequency, A values are quite robust and some data from all five high-miss periods are included. We therefore conclude that $A = 0.264 \pm 0.013$ s. Note that the standard deviation is less than 5% of the mean A value.

PBT distributions using A = 0.264 are used to estimate λ throughout the study period by following the procedure of Allen et al. in reverse order (248). Excluding the "high-miss periods" when the application of PBT distributions is not justified, hourly λ values range between 0.11 Hz and 15.1 Hz, with an average of 3.5 Hz. The best-fit B and C values are also calculated according to Allen et al. (248), but the C value is not statistically significant due to smaller folder limits used during CRPAQS (500 spectra per folder) relative to the BIIS (1000). We use our best-fit B value of 0.264 s, and a C value of 0.00024 s taken from laboratory experiments conducted under similar conditions (H. Furutani, Personal Communication). The difference between the A values from this study and previous studies is attributed to a change in the ATOFMS data acquisition mode. ATOFMS can be operated in either non-wide dynamic range (non-WDR) or wide dynamic range (WDR) data acquisition mode (255). When connecting two identical digitizers via a signal splitter to the signal source and attenuating one digitizer (30 db), WDR mass spectra (signal level ranging from 0 to 8000 instead of 0 to 255) can be obtained by combining the two signals (256). Although operating ATOFMS in WDR mode produces mass spectra with a much greater dynamic range, it requires significant computer time and significantly increases both the A and B values. During the current study, WDR spectra were acquired for positive ions, leading to a value of A that is higher than that in previous work when only non-WDR spectra were acquired (248). The lab experiments also support our conclusion that A and B are comparable when operating in WDR mode, since the most time-consuming process in obtaining single particle data is the data transfer from the acquisition board to the computer; the actual data saving time represents only a minor fraction of the data transfer process.

2. Scaling of ATOFMS Measurements with MOUDI Measurements

Scaled mass concentrations are calculated based on the effective sampling duration which excludes instrument busy time and offline periods. After obtaining ATOFMS busy time parameters, ATOFMS hit and missed particle information was processed for comparison with the MOUDI measurements. Hit particles were binned into size and time bins matching the MOUDI data. The MOUDI size bins are: 0.18 – 0.32, 0.32 – 0.56, 0.56 – 1.00, and 1.00 – 2.50 μm. The time frame is limited to the six MOUDI IOPs listed above. A total of 24 time-size bins are considered in the comparison, but data from two bins are excluded from the scaling procedure for the following reasons: (a) the MOUDI mass concentration was less than twice the mass uncertainty in the 1.00-2.50 μm bin on 31 January 1000 – 1600, indicating high uncertainty in the MOUDI measurement; and (b) the total number of hit particles by ATOFMS in the 0.18-0.32 μm bin on 1 February 0500 – 1000 was less than 100, which is deemed too few for a statistically representative measurement. Ultimately, mass concentrations in 22 bins were compared for quantitative analysis. Single particle sizes and counts were collected for each bin within the specified size range and time range. Using the measured flow rate through the instrument, an ATOFMS total particle mass concentration was calculated for each bin assuming all the particles were spherical. Morawska and coworkers obtained an overall average ambient submicron particle density of 1.7 $g \cdot cm^{-3}$ (257). The average density of supermicron particles would be even higher due to the increased fraction of sea salt and dust particles which have densities of 1.9 $g \cdot cm^{-3}$ and 2.7 $g \cdot cm^{-3}$, as reported by Hänel and Thudlum (258). Thus we use a density of

1.9 g·cm^{-3} for all $PM_{2.5}$ particles in mass concentration calculation instead of the 1.3 g·cm^{-3} value used in previous work (85,154,248,249). The scaling factor, ϕ_{MOUDI}, was constructed as the parameter to compensate for the difference between ATOFMS and MOUDI measurements. ϕ_{MOUDI} represents the inverse of the ATOFMS

particle detection efficiency and is defined with the following expression:

$$\phi_{MOUDI} = \frac{m_{MOUDI}}{m_{ATOFMS}} \tag{5.3}$$

where m_{MOUDI} is MOUDI mass concentration, and m_{ATOFMS} is ATOFMS mass concentration before scaling. ϕ_{MOUDI} is a function of particle size and can be expressed with a power law relationship with D_a:

$$\phi_{MOUDI} = \alpha \cdot D_a^{\beta} \tag{5.4}$$

where α and β are the best-fit parameters determined by non-linear regression of m_{MOUDI} on m_{ATOFMS} over all 22 bins. Physically, 1/α is the particle detection efficiency for a 1.0 μm particle and β represents the degree to which particles with sub-optimal sizes are deflected from the centerline in the ATOFMS inlet. Based on Equation (5.4), it is clear that varying the density value will not affect the scaled results; only the scaling parameters will change. The best-fit values of α and β are 1747.52 ± 363.96 and−4.41 ± 0.28 for this study, so ϕ_{MOUDI} varies from 3.4×10^6 for a 0.18 μm particle to 31 for a 2.5 μm particle.

Upon obtaining α and β, the value of ϕ_{MOUDI} was calculated for every single particle using Equation (5.4) based on the measured particle diameters by ATOFMS. The following equation was used to calculate scaled ATOFMS mass concentrations:

$$m_{ATOFMS-MOUDI} = \sum_i \phi_{Da,i} \cdot m_i \tag{5.5}$$

where $m_{ATOFMS\text{-}MOUDI}$ is the ATOFMS mass concentration after scaling with MOUDI, ϕ and m_i are the scaling factors and mass concentrations for each single particle respectively. Comparison of the scaled ATOFMS and the MOUDI mass concentrations for all 22 bins results in an R^2 value of 0.85 as shown in **Figure 55**, indicating that two parameters (α and β) are sufficient to explain 85% of the variability in ATOFMS transmission efficiencies over the 0.18 – 2.5 μm D_a range during 6 different IOPs. It is important to note that the high R^2 value would not have been obtained if busy-time corrections had not been applied. Note the mass concentrations for the non-IOP periods can be calculated with the same scaling function at higher temporal resolution (1 hour) if one assumes that the ATOFMS scaling factors do not change over time. There is some uncertainty associated with this assumption, so scaling with real-time particle concentration measurements may be favorable for obtaining total mass concentrations as described in the next section.

3. Comparison between MOUDI Scaled ATOFMS Measurements and BAM Measurements

Both hourly BAM and hourly TEOM $PM_{2.5}$ mass measurements were made at the Fresno site. Because the TEOM inlet was heated to 50 ºC during sampling in order to remove interferences from water, other semivolatile compounds were also removed (259), yielding values that were systematically lower than the co-located BAM measurements by an average of 42%. Therefore, since ATOFMS does not remove water or semivolatile compounds to a significant extent due to short analysis times, hourly BAM mass concentration measurements (m_{BAM}) were chosen as the reference mass concentration to evaluate $m_{ATOFMS\text{-}MOUDI}$ for the entire study period as shown in

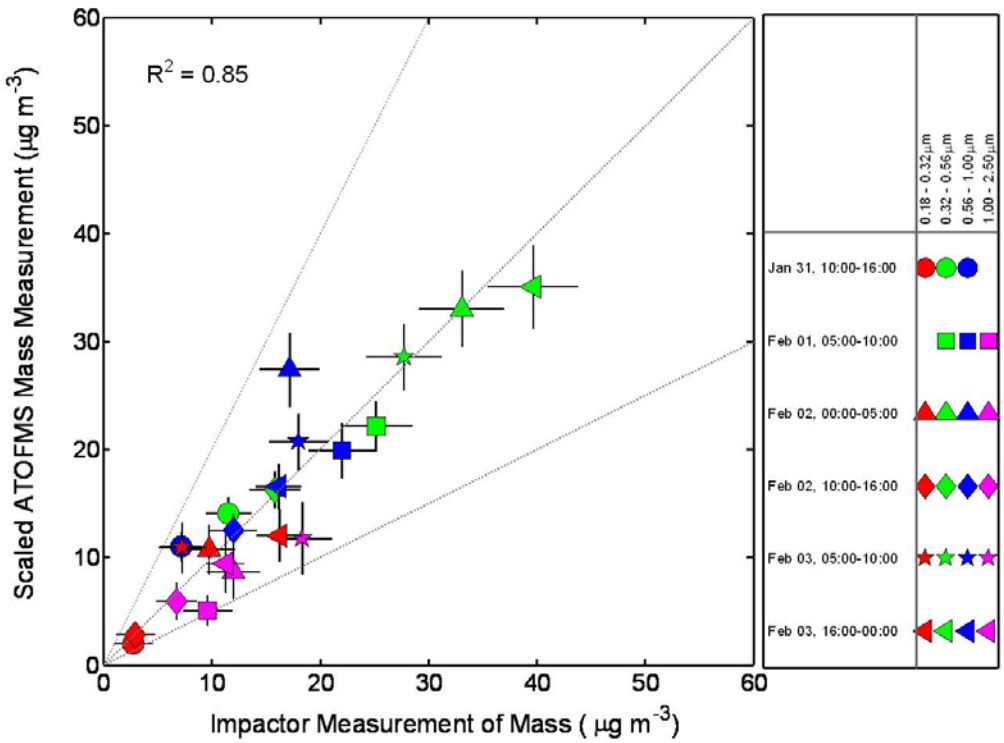

Figure 55: Comparison of scaled ATOFMS mass concentrations and MOUDI measurements in Fresno.

Figure 56. Both mass concentration measurements show distinct diurnal temporal variations, reaching maxima and minima at nearly the same time each day. Particulate matter concentrations remained relatively low during the day and increased substantially at night in Fresno during this study. The correlation between m_{BAM} and $m_{ATOFMS\text{-}MOUDI}$ is notably high with a R^2 value of 0.79. However, **Figure 56** also shows that $m_{ATOFMS\text{-}MOUDI}$ is systematically lower (about 30% less) than m_{BAM}. The ratio of mean values between these two measurements is 0.69 over the 26-day sampling period of interest. Several factors account for this difference. First, particles below 0.20 µm are not included in the $m_{ATOFMS\text{-}MOUDI}$ value as this represents the lowest size detectable by the ATOFMS instrument used in this study. An analysis of the MOUDI data during the six IOPs of interest indicates that particles larger than 0.18 µm make up 86% of the total $PM_{2.5}$ mass summed over all impaction stages from 0 - 2.5 µm (Σm_{MOUDI}). Second, the mean value

of m_{MOUDI} during the six IOPs is only 88% of the mean value of m_{BAM}. These two factors alone make it so the value of $m_{ATOFMS\text{-}MOUDI}$ cannot exceed 76% of the m_{BAM} value (0.86 × 0.88 = 0.76). Furthermore, the scaling function derived from the six IOPs most likely varied during the 26-day period. Thus, these factors result in the absolute values of $m_{ATOFMS\text{-}MOUDI}$ being 30% lower than the m_{BAM} values.

b. Scaling with the APS

1. Scaling ATOFMS Measurements with APS Measurements

Another quantification approach involves comparison of the ATOFMS particle counts at Angiola with particle number concentrations acquired with a co-located APS. Although APS measurements are not able to provide mass concentrations of individual chemical species like the MOUDI, they can provide particle number concentrations with

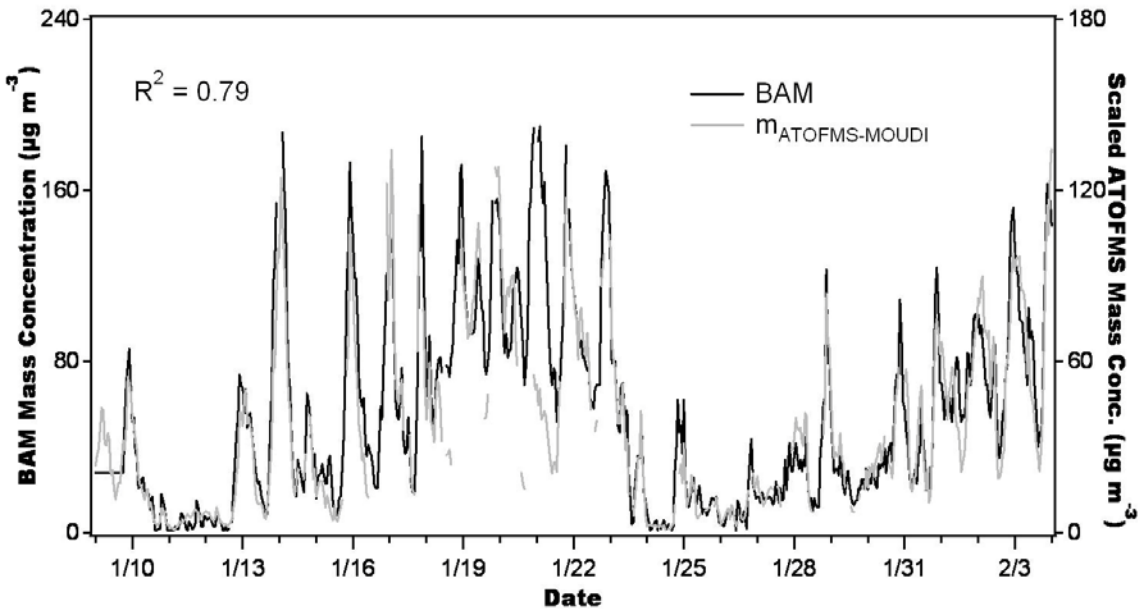

Figure 56: Temporal variation of hourly BAM and scaled ATOFMS PM2.5 mass concentrations in Fresno. The scaling function for the ATOFMS was obtained by comparison with MOUDI measurements.

very high temporal and size resolutions. This high resolution reference data can potentially provide more accurately scaled ATOFMS mass concentrations.

To scale the ATOFMS data with APS measurements, we follow an approach similar to the MOUDI scaling method by deriving scaling functions to correct for ATOFMS particle undercounting. To take advantage of the high time resolution properties of both measurements, one scaling function was constructed for each hour of the entire study period. Within each hour, single particle number counts collected by both ATOFMS and APS were segregated into 12 size ranges: 0.300-0.523, 0.523-0.605 μm, 0.605-0.699, 0.699-0.807, 0.807-0.933, 0.933-1.077, 1.077-1.243, 1.243-1.435, 1.435-1.655, 1.655-1.911, 1.911-2.207, and 2.207-2.547 μm. These size bins were adapted directly from the APS size bins by combining pairs of adjacent bins between 0.523 μm and 2.547 μm so that higher ATOFMS hit particle counts could be obtained for each bin. The smallest APS bin (0.300 - 0.523 μm) is also included in this calculation.

When the smallest APS bin is not used, the results do not change substantially from the 12 bin scaling discussed below. Since scaling is performed hourly, the factors that affect ATOFMS sampling, such as busy time and instrument offline time, are accounted for implicitly. The scaling factor, ϕ_{APS}, is defined as the following:

$$\phi_{APS} = \frac{Count_{APS}}{Count_{ATOFMS}} \tag{5.6}$$

One scaling factor was acquired for each size bin with Equation (5.6) for each hour. Like the scaling factors used in MOUDI scaling, ϕ_{APS} is also size dependant. By plotting the scaling factors against D_a, a scaling curve can be constructed for particles with aerodynamic diameters below 2.5 μm. **Figure 57a** shows the hourly scaling curves for the ATOFMS instrument stationed at Angiola on February 3. The error bars are generally not significant except for those at 5:00 and 6:00 during which APS measurements showed variations. The instrument was offline between 13:00 and 14:00, and therefore no scaling curve for this time period is presented. In **Figure 57a**, we see that ϕ_{APS} varies substantially from hour to hour. In the largest size bin, this variation spans nearly one order of magnitude. Most of this variability results from differences in ambient particle concentrations leading to differences in instrument busy times (36). This result further emphasizes the importance of high time resolution (hourly) scaling. The scaling factors obtained with MOUDI measurements will not be as accurate as ϕ_{APS} due to the time and size resolution limit and will not be able to reflect short term ambient particle concentration changes. In general, the APS scaling curve reaches a minimum at 1.655 μm – 1.911 μm size bin (bin midpoint is 1.783 μm) due to the higher ATOFMS transmission efficiency of particles in this size range than others. Two scaling functions were obtained for each hour by fitting the scaling curve separately on each side of the minimum point. Examples of the fitting of the scaling curve are included in **Figure 57b** and **Figure 57c** for 22:00 on February 03, 2001. The scaling function for the size range of 1.783 μm and below was obtained by exponential regression and was extrapolated down to 0.2 μm to obtain the scaling factors for smaller particles in the mass concentration calculation. The scaling function for the size range above 1.783 μm was obtained by a 2nd order polynomial regression. Thus, each scaling function can be fully described with five parameters which are used to calculate ϕ_{APS} as shown in Equation (5.7):

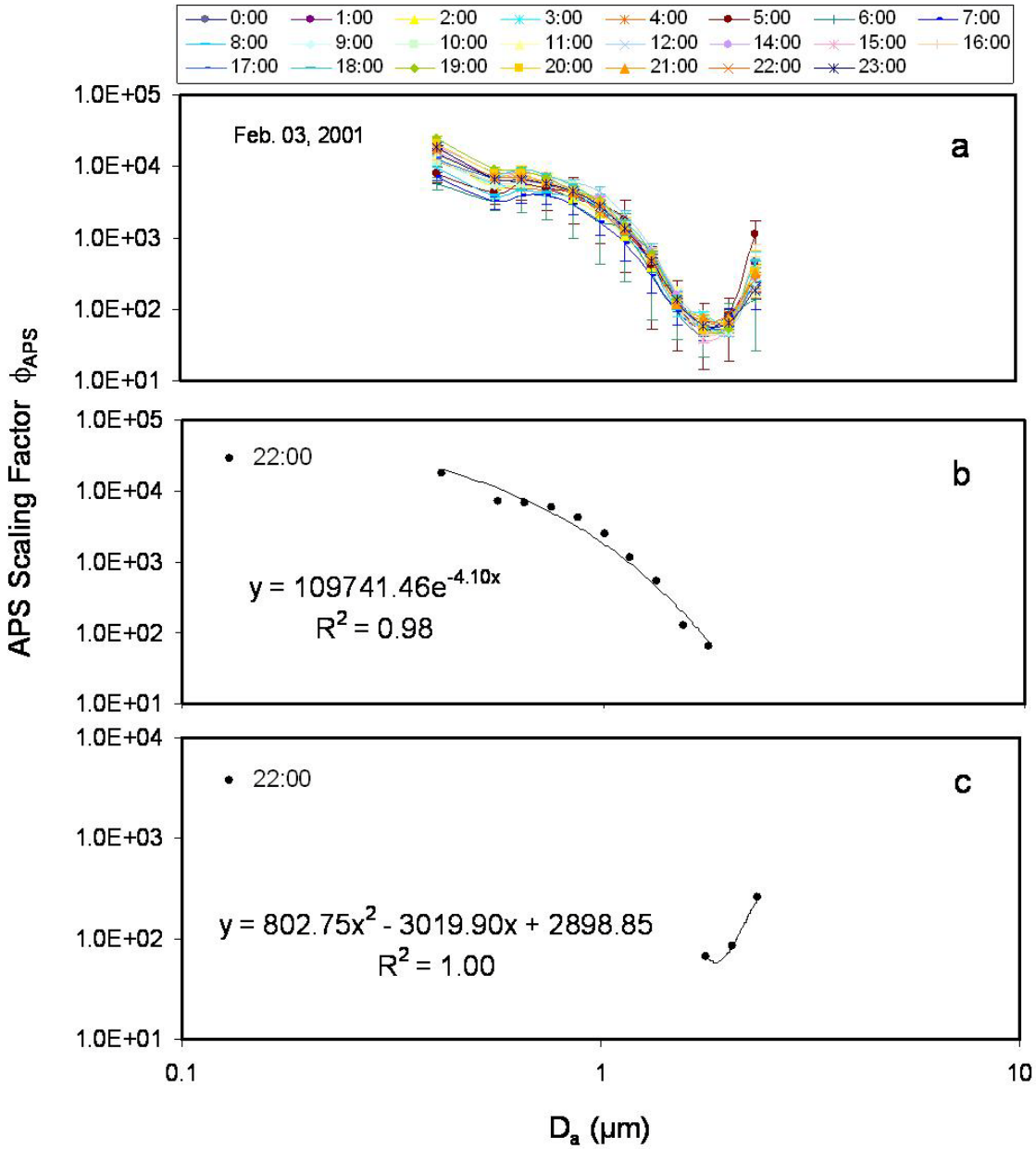

Figure 57: APS scaling curve for Angiola measurements. (a) hourly scaling curve for February 03, except for 13:00; (b) exponential regression of left half of scaling curve at 22:00; (c) polynomial regression of right half of scaling curve at 22:00

$$\phi_{APS} = \begin{cases} C_1 \cdot e^{C_2 \cdot D_a} & (when\ D_a < 1.783\ um) \\ C_3 \cdot D_a^{\ 2} + C_4 \cdot D_a + C_5 & (when\ D_a \geq 1.783\ um) \end{cases} \tag{5.7}$$

Five parameters were obtained for each hour of data collected at Angiola to correct ATOFMS measurements with APS measurements, generating number concentrations with 1 hour temporal resolution. The form of Equation (5.7) will allow a similar relationship to be applied other studies to obtain APS scaling factors.

With the scaling functions acquired, quantitative ATOFMS mass concentrations ($m_{ATOFMS\text{-}APS}$) were calculated. The ϕ_{APS} value for each particle can be obtained using the

D_a measured and the time when the datum was acquired. $m_{ATOFMS\text{-}APS}$ is calculated with the following equation knowing the instrument nozzle flow rate and assuming particles are spherical:

$$m_{ATOFMS-APS} = \sum_i \frac{M(D_{a,i}) \cdot \phi_{APS}(D_{a,i})}{V_{ATOFMS}} \tag{5.8}$$

where $M(D_{a,i})$ is the mass of each particle and V_{ATOFMS} is the volume of flow within each time period. Equation (5.8) makes it possible to construct quantitative particle mass concentration information for individual particle classes with any size and temporal resolution from ATOFMS measurements assuming no preferential transmission of certain particle classes. Unlike MOUDI scaling, $m_{ATOFMS\text{-}APS}$ is sensitive to assumed particle density values. Rather than assuming all particles have the same density, we may assign different density values to particles with different sizes or chemical compositions for improved estimates of the total mass concentration.

2. Comparison between BAM Measurements and APS Scaled ATOFMS Mass Concentrations Obtained with Different Density Values

The most straightforward approach to obtaining mass concentrations from ATOFMS data is to assign a single density value to all particles. **Figure 58a** shows the correlation between m_{BAM} and $m_{ATOFMS\text{-}APS}$ when utilizing fixed density values of 1.8 $g{\cdot}cm^{-3}$, 1.9 $g{\cdot}cm^{-3}$, and 2.0 $g{\cdot}cm^{-3}$, respectively, for APS scaling. The slope of each regression represents the ratio of mean values between m_{BAM} and $m_{ATOFMS\text{-}APS}$. The value for $m_{ATOFMS\text{-}APS}$ shows the best agreement with m_{BAM} is obtained when utilizing a density of 1.9 $g{\cdot}cm^{-3}$ (shown in red in **Figure 58a**). The temporal variations of the above two mass concentrations are presented in **Figure 59**. They track each other extremely well with an R^2 value of 0.91. The Angiola aerosols were aged and dominated by carbonaceous aerosols with significant quantities of nitrate and ammonium associated with them. Based on ATOFMS chemical analysis, more than 80% of Angiola particles were aged carbonaceous particles. As particles age, they become more internally mixed aerosols composed of organic carbon, ammonium, nitrate, sulfate, and water, and in general, the particle-to-particle chemical variability decreases over time. Thus the good agreement between ATOFMS mass concentrations scaled with a single density and BAM measurements is most likely due to the chemical homogeneity of aged ambient aerosols. When applying the above method to scale ATOFMS measurements in a region where fresh emissions occur and many distinct particle types dominate, it is likely that applying one density value for all particles will not be sufficient.

Since ATOFMS measures the aerodynamic diameter of individual particle, it is possible to apply specific density values based on particle size. The unscaled ATOFMS

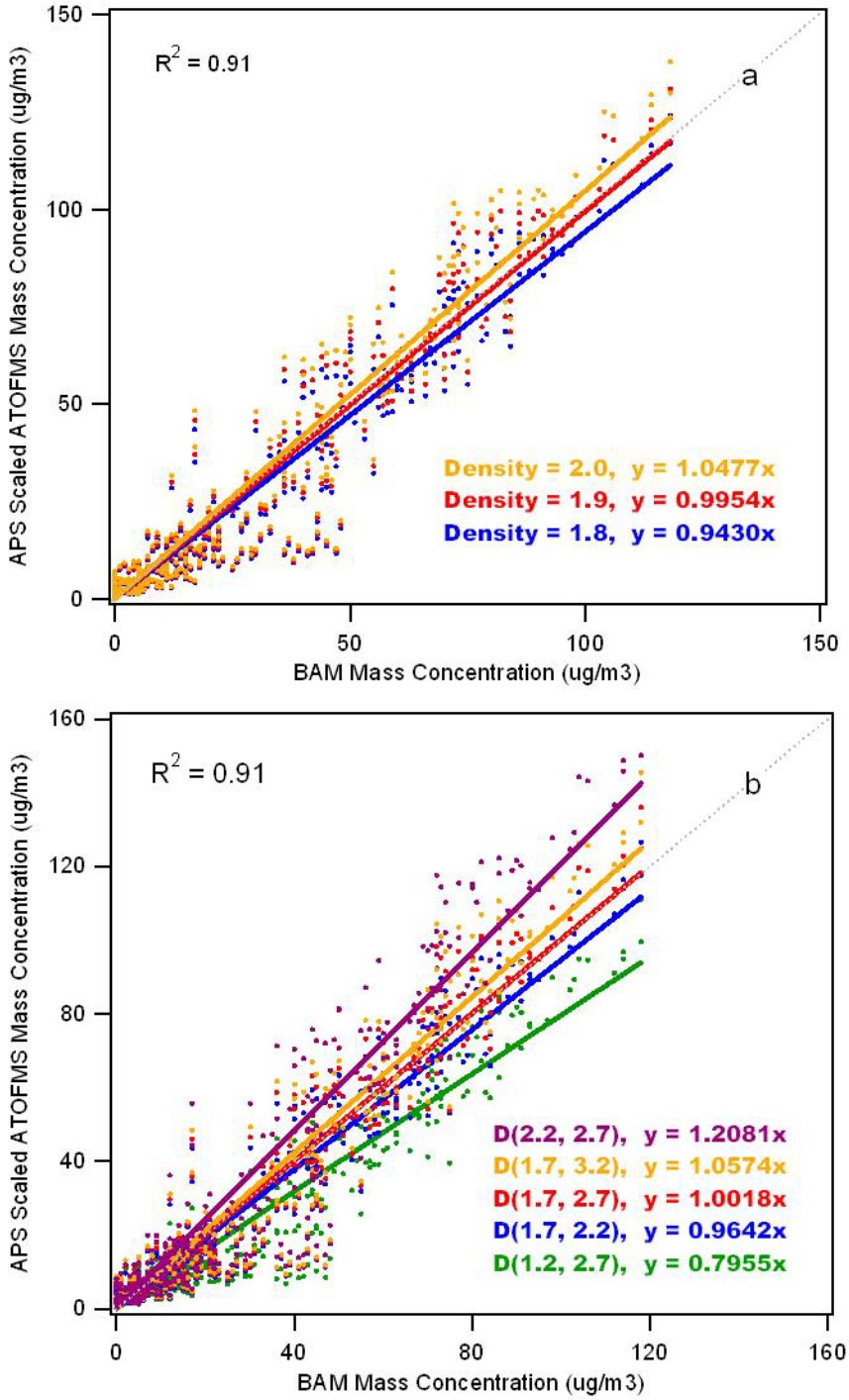

Figure 58: Correlations between BAM and APS scaled ATOFMS mass concentrations. (a) ATOFMS mass concentrations are obtained with single density (ρ) values for all particles (ρ = 1.8 g·cm^{-3}, ρ = 1.9 g·cm^{-3}, or ρ = 2.0 g·cm^{-3}); (b) ATOFMS mass concentrations are obtained with different density pairs for submicron and supermicron particles: 1.2 and 2.7 g·cm^{-3}, 1.7 and 2.2 g·cm^{-3}, 1.7 and 2.7 g·cm^{-3}, 1.7 and 3.2 g·cm^{-3}, and 2.2 and 2.7 g·cm^{-3}.

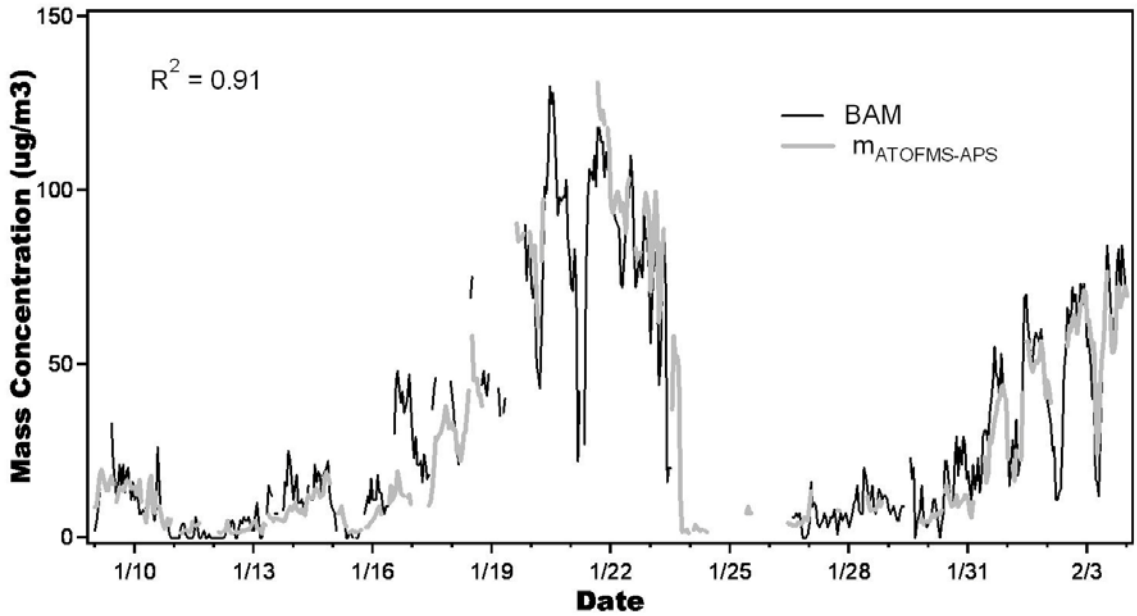

Figure 59: Temporal variation of Angiola particulate mass concentrations obtained with BAM and APS scaled ATOFMS (ρ = 1.9 g·cm^{-3}).

ambient particle size distribution shows that particles smaller than 1.0 μm in aerodynamic diameter account for a large portion of total particle numbers in Angiola. ATOFMS chemical composition measurements have shown that particles smaller than 1.0 μm are mainly carbonaceous particles with associated secondary inorganic components, while the relative fraction of inorganic particles increases substantially above 1.0 μm (156). Thus we segregate particles into two size ranges: submicron (0.2 < Da < 1.0 μm) and supermicron (1.0 ≤ Da < 2.5 μm). We use literature value of 1.7 g·cm^{-3} as the density for submicron particles (257), and 2.7 g·cm^{-3} for supermicron particles, an intermediate value for the various chemical components reported in this size range (258). The scatter plot between $m_{ATOFMS\text{-}APS}$ acquired with this pair of density values and m_{BAM} is included in **Figure 58b** (in red). Scaled ATOFMS and BAM mass concentrations track each other very well with a high correlation coefficient of 0.91. The absolute values are quite close to one another and nearly on top of the 1:1 line. We also varied the densities by 0.5 g·cm^{-3} in both directions for the sub- and super-micron particles separately. The correlations between each of these density pairs with the BAM measurements are also included in **Figure 58b**. The correlation values remain high (R^2 ~ 0.91) in all cases and only the ratios between $m_{ATOFMS\text{-}APS}$ and m_{BAM} are different. From the change in slope it is apparent that the total scaled ATOFMS mass concentrations are more sensitive to the submicron particle density than the supermicron particle density. This is due to the fact that the majority of the Angiola particle mass is in the submicron size mode.

We can go beyond just using size information and utilize chemically specific density values applied to each different particle type to obtain scaled ATOFMS mass concentrations. To convert from number to mass concentrations, we used the density value of 1.9 g·cm^{-3} for carbonaceous particles, 2.7 g·cm^{-3} for dust particles, 1.9 g·cm^{-3} for Na rich salt particles, 2.0 g·cm^{-3} for biomass emission particles and EC rich particles, and 1.9 g·cm^{-3} for the rest of the particle types (258,260,261). The multi-density scaled

ATOFMS mass concentrations also show a strong and very similar correlation with BAM measurements with a high R^2 of 0.91. As discussed earlier in this section, the advantages of utilizing various density values for each chemical composition are not fully realized in this particular study due to the fact that Angiola ambient particles are aged and thus very chemically homogeneous. In regions or seasons with more fresh emissions, it will most likely become necessary to assign chemically specific density values for individual particle types. Additional lab and field investigations are underway to develop universal scaling factors that use specific density and shape factors for each particle type.

c. $PM_{2.5}$ Measurement Intercomparison

A number of different continuous particle measurements were available in both Fresno and Angiola during the CRPAQS. Thus it is possible to compare the correlations among different measurements. Such comparisons are helpful for evaluating the different methods used for scaling the ATOFMS mass concentrations. At the Fresno site, the available continuous $PM_{2.5}$ measurements are BAM, TEOM, Dust Aerosol Monitor (DAM), Nephelometer, Aethelometer, and $m_{ATOFMS\text{-}MOUDI}$. Several hours of nephelometer data points were removed in the morning periods of January 30, January 31 and February 1 due to the extraordinarily high uncertainties in nephelometer measurements. The continuous $PM_{2.5}$ measurements for the Angiola site include BAM, nephelometer, aethelometer, and $m_{ATOFMS\text{-}APS}$ with density values of 1.9 $g{\cdot}cm^{-3}$ for all particles. Although the measurements of all these instruments represent the total $PM_{2.5}$ particle mass concentrations, each instrument is based on a different theory and has its own strengths and weaknesses. Therefore, it is quite reasonable to expect the correlation between any two measurements to be less than 1 (262).

The correlation coefficients between every pair of measurements are tabulated in **Table 9** for both Fresno and Angiola. For Fresno site comparisons, using an R^2 value of 0.7 and above to represent a good correlation, only the BAM measurement shows a fairly good correlation with all the other measurements with correlation coefficients ranging from 0.73 – 0.93. The TEOM measurement only correlates well with BAM and aethelometer measurements. This suggests that in this environment, the heated TEOM does not provide measurements of mass concentrations that are as accurate as those of the BAM. The $m_{ATOFMS\text{-}MOUDI}$ correlates well with the BAM, DAM, and nephelometer measurements. The overall correlation for MOUDI scaled ATOFMS $PM_{2.5}$ mass concentrations is as good as most other $PM_{2.5}$ measurements in Fresno. Similarly, Angiola correlation comparisons are shown in **Table 9b**. The BAM, nephelometer, and $m_{ATOFMS\text{-}APS}$ measurements show high correlation coefficients of greater than 0.90. The aethelometer measurements differ substantially and show lower correlation coefficients with the other three measurements. The strong correlation of ATOFMS mass concentrations with other $PM_{2.5}$ measurements provides support that the ATOFMS data can be scaled using peripheral instruments, such as the APS, to provide a measure of real ambient particle mass concentrations. The ultimate goal in developing this scaling procedure is not to just provide total $PM_{2.5}$ mass concentrations since these can be

(a)

Fresno R^2	BAM	TEOM	DAM	NEPH	AETH	ATOF-M
BAM	1.00	0.86	0.93	0.75	0.79	0.79
TEOM	0.86	1.00	0.59	0.60	0.94	0.64
DAM	0.93	0.59	1.00	0.70	0.53	0.78
NEPH	0.75	0.60	0.70	1.00	0.58	0.81
AETH	0.79	0.94	0.53	0.58	1.00	0.62
ATOF-M	0.79	0.64	0.78	0.81	0.62	1.00

(b)

Angiola R^2	BAM	NEPH	AETH	ATOF-N
BAM	1.00	0.92	0.60	0.91
NEPH	0.92	1.00	0.77	0.93
AETH	0.60	0.77	1.00	0.63
ATOF-N	0.91	0.93	0.63	1.00

BAM: beta attenuation monitor
DAM: dust aerosol monitor
NEPH: nephelometer
AETH: aethelometer
TEOM: tapered element oscillating microbalance
ATOF-N: APS scaled ATOFMS mass concentrations
ATOF-M: MOUDI scaled ATOFMS mass concentrations

Table 9: Correlation coefficients of $PM_{2.5}$ measurements. (a) Fresno site. (b) Angiola site.

measured using a variety of other dedicated techniques, but instead to use ATOFMS to provide mass concentrations of particles from specific sources. Thus, this study represents a critical step in the development of the most appropriate scaling procedures that will allow us to use ATOFMS to obtain quantitative source apportionment results in future studies.

iv. Conclusions

In this paper, we compare two methods for scaling ATOFMS measurements using reference measurements to obtain quantitative particle mass concentrations. By comparing ATOFMS single particle measurements with MOUDI mass measurements, we obtain scaled ATOFMS mass concentrations that correlate well ($R^2 = 0.79$) with a BAM, which serves as an independent mass concentration reference method. However, the absolute values of scaled ATOFMS mass concentration is only close to MOUDI measurements during the IOPs within the specified size range. Reduced ratios between the scaled ATOFMS and BAM mass concentrations are obtained when applying the scaling function to other periods during the study. Increasing the time resolution of the scaled ATOFMS mass concentrations to 1 hour (i.e. shorter than that of the MOUDI which is 5-8 hours) also introduces uncertainties. Both of these factors result in the absolute values of scaled ATOFMS mass concentration being only 70% of those measured by the BAM over the full study. Some of this difference can be explained by the underestimation of particles smaller than 0.18 μm by ATOFMS. The main advantage of scaling with the MOUDI measurements is to obtain size segregated mass concentrations of individual chemical species, making it possible to derive relative sensitivity factors (85).

APS measurements provide high temporal resolution particle number concentrations. By scaling ATOFMS particle counts with the APS and applying composition specific density values to the ATOFMS particle types, we are able to obtain ambient particle mass concentrations that correlate extremely well with BAM measurements ($R^2 = 0.91$). Future papers will address using chemically specific scaling factors which correct for density and shape factors.

In conclusion, continuous and quantitative ambient particle mass concentrations can be obtained from ATOFMS measurements by scaling with measurements from a co-located MOUDI or APS. The MOUDI method should be used if one is interested in deriving chemical sensitivity factors for different species. If one is more interested in real-time variations in particle mass concentrations (i.e. from different sources), the APS method is a more appropriate choice. The use of these methods for scaling extends ATOFMS to a more quantitative tool for studying ambient aerosol composition, transformations, and reaction mechanisms. When applying these scaling methods to individual particle types measured by the ATOFMS and correcting for chemical differences, quantitative mass concentrations of individual particle (or source) types with high time and size resolution can be obtained. The ultimate goal is use these scaling procedures to obtain quantitative mass fractions of particles from different sources in future ambient source apportionment studies.

v. Acknowledgements

We thank the California Air Resources Board for financial support (Contract No. 04-336) and the SJV funding agency for supporting CRPAQS. We also thank Dr. Hiroshi Furutani for sharing his busy time results and Dr. William Vance of ARB for a careful critique of this manuscript.

8. The Effect of APS Scaling Functions on the Quantification of Aerosol Time-of-Flight Mass Spectrometry Measurements

i. Introduction

Traditionally, particulate matter is characterized with off-line filter/impactor based techniques, which normally require long sampling durations and labor-intensive analysis. Newly developed real-time particulate mass measurements, like the beta attenuation monitor, the tapered element oscillating microbalance, the Dusttrak sampler, and the continuous aerosol mass monitor, are able to provide high temporal resolution of particulate matter mass concentrations by utilizing the absorbing or scattering properties of the particles; however, no information on individual chemical species can be obtained from these methods (263-266).

Real-time single particle mass spectrometry (RTSPMS) measurements are able to overcome many disadvantages of the above techniques and provide continuous on-line particulate matter measurements (243,244,267). Despite the fact that extensive information on individual particle size and chemical composition can be acquired with RTSPMS measurements, it has been a challenge for these methods to provide quantitative aerosol mass concentrations. Most of the RTSPMS measurements introduce particles into a vacuum from atmospheric pressue via a supersonic expansion through an orifice. During transmission into the reduced pressures of a mass spectrometer, only a certain fraction of the particles are able to reach the center of the ionization region and become ionized (173). In order to compensate for these transmission losses, efforts are made to scale the data to obtain quantitative number or mass concentrations of ambient particles (30,36,85,249,250,268,269).

In a recent study, Qin et. al demonstrated the ability to obtain high temporal and size resolved quantitative particulate matter mass concentrations from ATOFMS measurements by scaling with reference methods (157). ATOFMS measurements provide the aerodynamic diameter and mass spectra of individual particles in real-time, enabling the study of particle transformation, mixing state, and source apportionment. One of the reference methods used for this study was an aerodynamic particle sizer (APS) which measures number concentrations for sizes between 0.2 and 2.5 μm. APS acquires real-time particulate aerodynamic size distribution by accelerating particles to different size-dependant terminal velocities which can be calculated with particle time-of-flight through the scattering lasers (254). By comparing ATOFMS and APS measurements for individual size ranges, a size dependant scaling function can be constructed, which is further used to acquire a scaling factor for each particle. The scaling factor represents the degree that ATOFMS undercounts particles for different sized particles. By multiplying ATOFMS measurements by scaling factors to correct for undercounting, a true representation of the ambient aerosols without biases due to transmission losses can be obtained . Qin and co-workers demonstrated that the APS scaled ATOFMS mass concentrations strongly correlate with independent beta attenuation monitor mass measurements, effectively providing quantitative particulate matter mass concentrations (157). The above scaling method also enables one to obtain the mass concentrations of

individual ATOFMS particle classes, assuming no preferential transmission of particles in each type and similar detection efficiencies.

The procedure used by Qin et al (2006) works well when APS data are available. A question arises as to how to scale ATOFMS data when no APS is available in a study. One also might ask whether this approach for scaling is universal and can be applied to all field studies with an ATOFMS. In this paper, the ATOFMS measurements from two field studies were scaled with APS scaling functions from five different field studies to study the effect of using different scaling functions on the scaling results. The ATOFMS data from the two test studies were acquired during the California Regional Particulate Air Quality Study (CRPAQS) in Fresno and Angiola (270). The five reference studies that provided APS scaling functions from a broad range of ambient conditions and aerosol types are the: Texas Air Quality Study in 2000 (TexAQS) (271), North Carolina Ambient Coarse Particle Concentrator Characterization Study (NC-CCS) (268), Cloud Indirect Effects Experiment (CIFEX) (272), UCSD Freeway Study (Freeway) (273), and Atmospheric Brown Clouds Post-Monsoon Experiment (APMEX) (274). Co-located APS data were also available during the Angiola study, which will be used to compare the results between using scaling functions from both the same study and the reference studies.

ii. Experimental

All studies including Angiola, TexAQS, NC-CCS, CIFEX, Freeway, and APMEX had side-by-side ATOFMS and APS measurements, except for the Fresno study where no APS measurements were made. A TSI APS Model 3320 was used during the TexAQS and Angiola studies, and Model 3321 was used for all other studies (TSI, Minnesota). The details of the transportable ATOFMS have been described by Gard and co-workers (127).

a. CRPAQS ATOFMS Measurements and Data Analysis

California's San Joaquin Valley is one of the most polluted areas of the country, experiencing extremely high particulate matter mass concentrations throughout the winter season due to the stagnant meteorological conditions (275). In order to better understand particulate matter pollution and identify major emission sources, a multi-year, multi-agency field campaign, the California Regional Particulate Air Quality Study (CRPAQS), was deployed at selected locations in the valley (172,276-279). Two ATOFMS were operated continuously in Fresno and Angiola from November 30, 2000 to February 4, 2001 as part of the CRPAQS to study wintertime aerosol composition, transformations, mixing state, and source apportionment. The size and chemical composition of more than 2 million particles was acquired with ATOFMS at each site. The data collected between January 9th, 2001 and February 4th, 2001 will be scaled with reference APS scaling functions to study the effect of different scaling curves on ATOFMS scaling results. Particles with diameters 0.2 – 2.5 µm were the focus of this study.

Custom software was used to calibrate the mass spectra and extract ion peaks into peak lists. These peak lists were imported into a single particle mass spectrometry data analysis tool kit, YAADA, for extensive analysis (160). The spectra were then classified with an adaptive resonance theory based clustering method (ART-2a) (35), which groups particles into clusters based on the existence and intensity of ion peaks in individual

particle mass spectra. Single particle mass spectral information is converted into a weight matrix for classification. Two particles are considered to belong to the same cluster if the dot product of their weight matrices is higher than a pre-determined threshold value, which was set to 0.8 for the current work. Upon applying ART-2a on the CRPAQS datasets, major particle types that accounted for 90% of total particles were isolated for further analysis. The majority of the single particle mass spectra contain information on both positive and negative ions, however, about 5.9% of the particles in Fresno study and 1.5% of the particles in Angiola study did not produce positive mass spectra. These particles were excluded from the classification step.

b. Reference Studies with APS Scaling Functions

APS scaling functions from five reference studies, including TexAQS, NC-CCS, CIFEX, UCSD Freeway, and APMEX were applied to the Fresno and Angiola ATOFMS measurements to study the impact of using multiple scaling functions.

TexAQS is a comprehensive research project to address the air pollution problems in the state of Texas, as a result of the high number of days in exceedance of the national 1-hour standard of ozone and fine particulate matter concentrations (271). The goal of this study is to investigate ground level ozone and fine particulate matter in the Houston region and the east half of Texas to determine whether the pollutants are from local sources or long-range transport. ATOFMS was operating continuously for 4 weeks from August 20 to September 15, 2000 at the La Porte airport, which is located 40 km east of downtown Houston. TexAQS measurements represent a polluted urban environment. The NC-CCS collected lab based ambient measurements at the EPA Human Studies Facility in Chapel Hill, NC in the summer of 2003. The main purpose of this study was to characterize the effect of the coarse particle concentrator on ambient particulate matter chemical composition and size distributions (268). During the first concentrator characterization study (NC-CCS-I), the ATOFMS was operated for 10 hours of switching between non-concentrated and concentrated ambient particles. ATOFMS was operated for 8 hours during the second concentrator characterization study (NC-CCS-II), a period when substantially higher (nearly 100%) ambient relative humidity (RH) was encounted which led to severe degradation in visibility. CIFEX was conducted in April 2004 at Trinidad Head, California to observe long range transport of Asian dust traveling across the Pacific Ocean (272). The sampling site is located on the coast of California about 60 miles south of the California-Oregon border. This study captured particles in a remote marine environment with occasional influence from local anthropogenic activities and long-range transport of Asian dust. The UCSD Freeway Study took place in the summer of 2004 where continuous ambient measurements were conducted with an ATOFMS for nearly 5 weeks inside a trailer at the University of California, San Diego (273). The sampling site was only 10 meters away from a major freeway with heavy traffic. The purpose of this measurement was to study the instantaneous chemistry of vehicular emission particles under ambient conditions, to aid in source apportionment of particles from vehicle emissions. Finally, during the APMEX, ambient ATOFMS sampling was conducted in October, 2004 at Hanimaadhoo, a very remote location near the north edge of the Maldives islands (274). The main

purpose of this study was to understand the atmospheric impact of anthropogenic activities.

c. The Calculation of the Scaling Functions in Reference Studies

The detailed APS scaling procedure is described in the recent paper by Qin and co-workers (157). The same method is adapted here with minor modifications. Briefly, particle number counts were first tabulated from both APS and ATOFMS measurements for the following 12 size ranges: 0.300-0.523, 0.523-0.605, 0.605-0.699, 0.699-0.807, 0.807-0.933, 0.933-1.077, 1.077-1.243, 1.243-1.435, 1.435-1.655, 1.655-1.911, 1.911-2.207, and 2.207-2.547 μm. A scaling factor is calculated for each size bin by calculating the ratio of APS to ATOFMS particle counts for the corresponding size range. By plotting the scaling factors against the mid point of each size bin, a scaling curve can be obtained which is used to fit the scaling functions. Since the purpose of the current work is to test the applicability of scaling functions from reference studies to test studies, generating hourly scaling functions from reference studies for the object studies is not applicable. Thus, only one average scaling function is obtained from each reference study in the current work. For each reference study, time periods were removed if either APS or ATOFMS were offline. Since scaling curves can change substantially at different times of the day due to the variation in ambient particle concentrations and compositions, an average scaling curve for the same hour of the day throughout the whole study period was first calculated. The final scaling curve was obtained by averaging the mean scaling curves for each hour of the day. Similar to the previous work by Qin et al., each scaling function is fitted separately for the size range below and above 1.783 μm which can be characterized with 5 parameters:

$$\phi_{APS} = \begin{cases} C_1 \cdot e^{C_2 \cdot D_a} & (when\ D_a < 1.783\ um) \\ C_3 \cdot D_a{}^2 + C_4 \cdot D_a + C_5 & (when\ D_a \geq 1.783\ um) \end{cases} \quad (1)$$

where C1 and C2 are the best-fit parameters determined by exponential regression of scaling factors over the size bins. The first function was extrapolated down to 0.2 μm to obtain the scaling factors for the smallest particles detected by ATOFMS. C3, C4, C5 were obtained by second-order polynomial regression.

iii. Results and Discussion

a. Scaling Curves and Scaling Functions

The scaling curves for the reference studies: TexAQS, NC-CCS-I, NC-CCS-II, CIFEX, Freeway, APMEX, and Angiola are presented in **Figure 60**. Since APS measurements are available during the Angiola study, the Angiola APS scaling curve is also included along with the reference scaling curves. All scaling curves resemble a reverse check mark in the $PM_{2.5}$ (Da ≤ 2.5 μm) size range with the lowest point at 1.783 μm for most curves. The exceptions are the NC-CCS curves which dip at 1.545 μm and the APMEX curve which dips at 2.059 μm. The scaling curves from all six studies are similar in shape but the absolute scaling factors can vary by several orders of magnitude. The APS scaling parameters for each study are listed in **Table 10**.

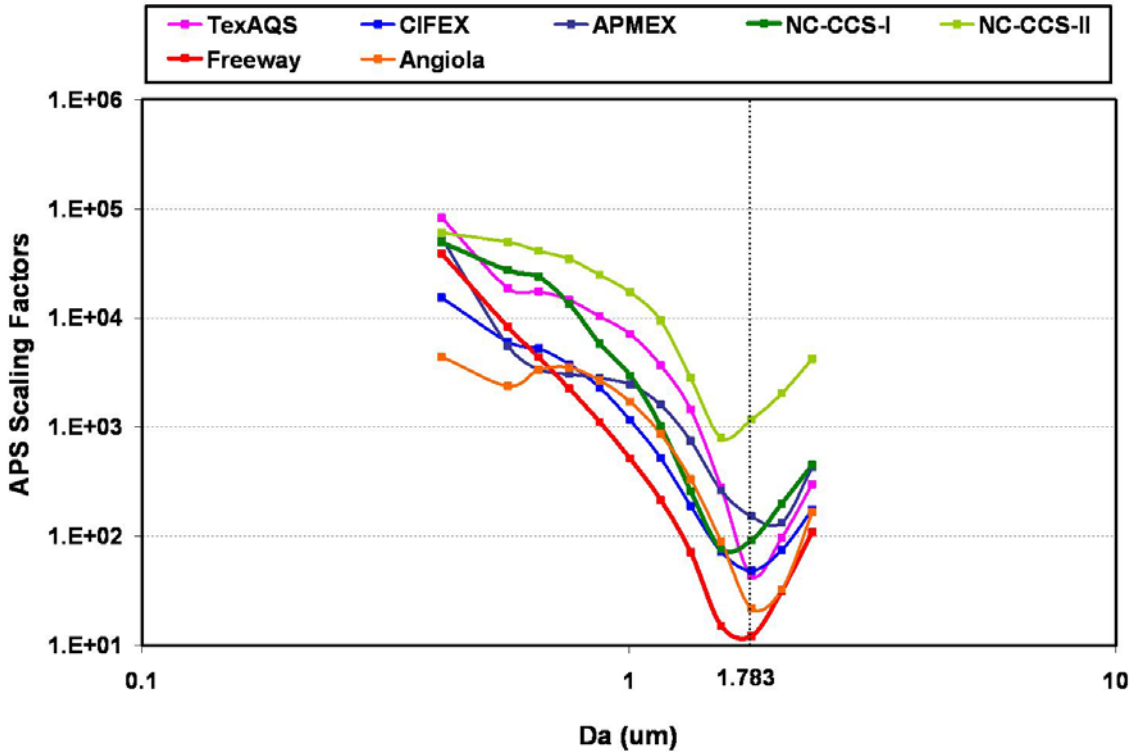

Figure 60: APS scaling curves for all studies, including TexAQS, NC-CCS-I, NC-CCS-II, CIFEX, Freeway, APMEX, and Angiola studies.

Table 10: APS scaling parameters for all studies.

Study	C1	C2	C3	C4	C5
CIFEX	90538.75	-4.42	372.61	-1336.04	1245.93
Freeway	241360.23	-5.96	289.94	-1043.43	950.88
TexAQS	598326.07	-4.91	742.50	-2658.89	2423.82
Angiola	41576.86	-3.81	635.66	-2403.85	2287.07
NC-CCS-I	558422.02	-5.33	682.05	-2233.29	1905.64
NC-CCS-II	381091.24	-3.46	6250.30	-20892.62	18551.49
APMEX	66592.45	-3.48	1674.69	-6501.40	6420.04

b. Major Particle Types in CRPAQS

Detailed discussions of the major particle types are provided in another paper by Qin and co-workers (270), and only a brief description is provided here. The majority of particles analyzed during the CRPAQS study were transformed, as indicated by the presence of secondary ammonium (m/z 18) and nitrate (m/z -46, -62 and -125) ion marker peaks in their mass spectra. OC represent particles mainly containing organic carbon with secondary ammonium and nitrate; biomass are organic carbon particles with

very intense potassium peak; HMOC represent organic carbon particles that contain characteristic peaks between m/z 100 and 200 in both positive and negative spectra (162); ECOC are particles containing both elemental carbon and organic carbon; EC represent elemental carbon particles with intense C_n^+/C_n^- peaks (n is integer); sea salt are freshly emitted sea salt particles with intense sodium and chloride peaks; aged sea salt are sea salt particles containing significant amount of nitrate and some organics; dust are inorganic mineral species mixed with nitrate and organic carbon; and NH_4NO_3-OC represent organic carbon particles but with huge amount of ammonium nitrate. All the aforementioned particle types are present in both the Fresno and Angiola studies. There are also particle types that are specific to each location.

Knowing the ATOFMS sample flow rate, the un-scaled particle type mass concentrations can be obtained from raw ATOFMS counts by assuming all particles are spherical with a density of 1.9 g/cm^3 (157). **Figure 61** shows the un-scaled daily average particle type mass concentrations and mass fractions in the size range of 0.2- 2.5 μm. The size resolution is 0.1 μm with the label representing the bin midpoint. The low mass concentration values within each bin (< 0.2 μg/m^3) illustrate the significant

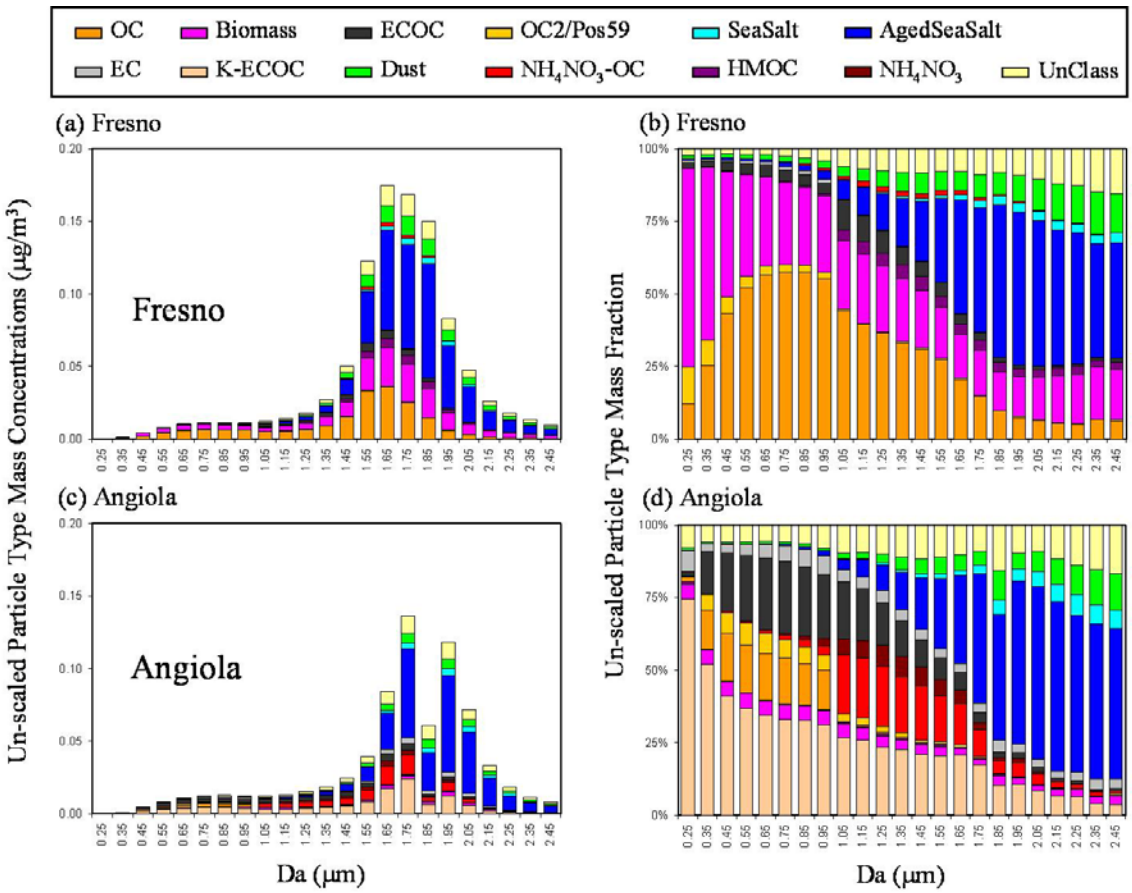

Figure 61: Size-resolved un-scaled particle type mass concentrations and mass fractions for Fresno and Angiola. (a) un-scaled particle type mass concentrations in Fresno (b) un-scaled particle type mass fractions in Fresno (c) un-scaled particle type mass concentrations in Angiola (d) un-scaled particle type mass fractions in Angiola.

undercounting of particles by the ATOFMS as shown in **Figure 61a** and **Figure 61c**. Without scaling, the ambient particle mass concentrations are centered near 1.5 – 1.9 μm. These size-resolved mass concentration distributions are not indicative of the atmospheric concentrations, but reflect the preferential transmission of particles around 1.7 μm by the ATOFMS nozzle. This preferential transmission is one aspect that can be corrected using APS scaling functions. Since particle transmission efficiency mainly depends on size (173), particles within the same size range are undercounted to the same extent. Therefore, the particle type mass fractions as a function of size shown in **Figure 61b** and **Figure 61d** represent the true ambient particle fractions without scaling..

The major particle type mass fractions illustrate that carbonaceous particles dominate the submicron size range ($0.2 \leq D_a < 1.0$ μm), however their fractions decrease substantially in the supermicron range ($1.0 \leq D_a \leq 2.5$ μm) as aged sea salt and dust particles becoming the dominant components. **Figure 61** also show that despite the fact that carbonaceous particles (mainly organic carbon, elemental carbon, and biomass) account for more than 90% of the total mass in the submicron size range at both sites, the percentages of biomass and OC particles are much lower in Angiola. The combined mass fractions of carbonaceous particles are similar in Fresno and Angiola, however, a lower fraction of biomass and a higher fraction of K-ECOC are observed in Angiola due to particle aging (270).

c. Scaled ATOFMS Mass Concentrations

Scaling causes a dramatic shift in the size distributions of major particle type mass concentrations compared to those shown in **Figure 61a** and **Figure 61c**.

Representative distributions after scaling are included in **Figure 62**. The y-axis represents the 24-hour

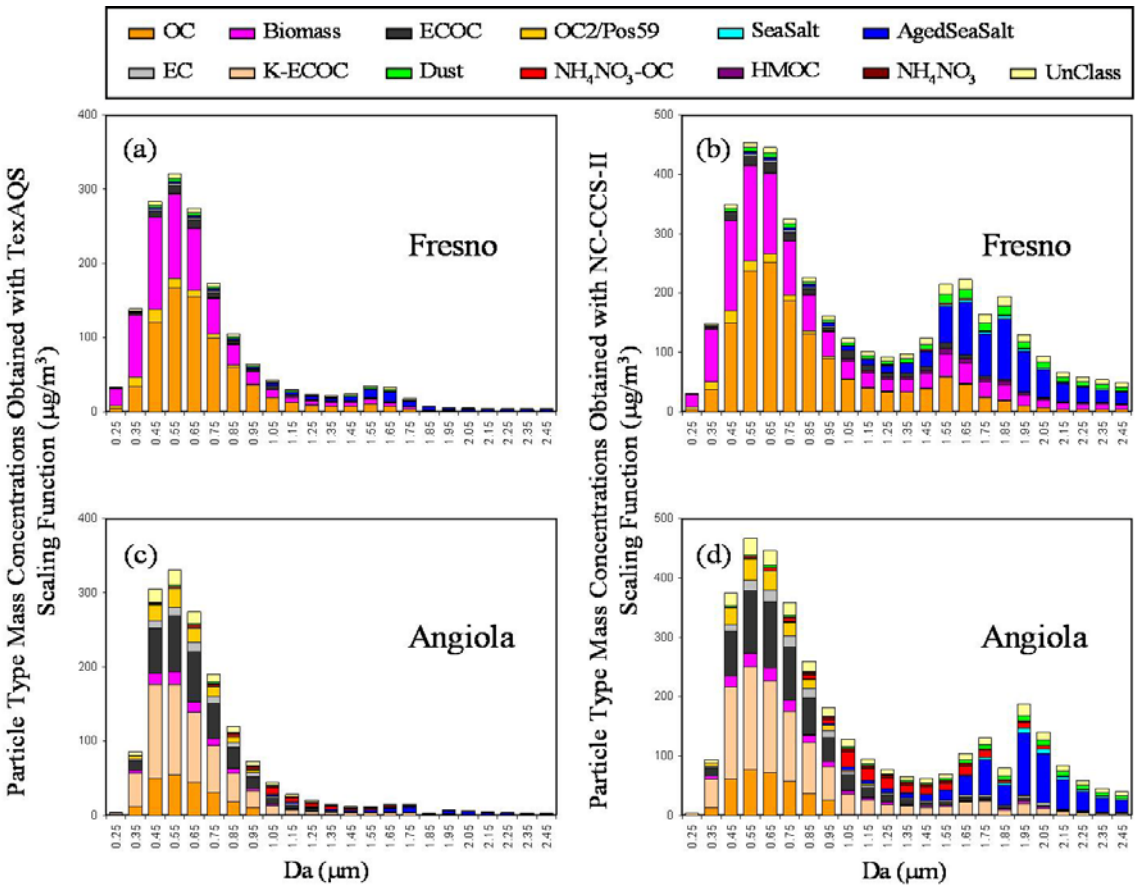

Figure 62: Fresno and Angiola size-resolved particle type mass concentrations scaled with TexAQS and APMEX scaling functions. (a) Fresno particle type mass concentrations with TexAQS APS scaling function (b) Fresno particle type mass concentrations with APMEX APS scaling function (c) Angiola particle type mass concentrations with TexAQS APS scaling function (d) Angiola particle type mass concentrations with APMEX APS scaling function.

average mass concentrations over the whole sampling duration; the x-axis shows the midpoint of each size bin with a resolution of 0.1 µm. **Figure 62a** and **Figure 62c** correspond to the scaled mass concentrations in Fresno and Angiola using the TexAQS APS scaling function. The total particulate mass concentration peaks between 0.5 - 0.6 µm with carbonaceous species dominating the submicron size range. The mass concentrations of aged sea salt particles increase in the supermicron range. Applying scaling functions from Freeway, CIFEX, and NC-CCS-I studies results in similar size distributions to those in **Figure 62a** and **Figure 62c**. **Figure 62b** and **Figure 62d** represent the scaled mass concentration of major particle types using APMEX scaling function. Compared to the results in **Figure 62a** and **Figure 62c**, the size distribution of APMEX scaled mass concentrations has an additional peak around 1.7 µm as well as the peak between 0.5 - 0.6 µm. The scaled mass concentrations calculated with the NC-CCS-II scaling function show similar distribution to that obtained with APMEX, except that the peak at 1.7 µm is a little more intense.

One major factor that affects the supermicron scaling results is the shape of the scaling curve. As shown in **Figure 60**, neither APMEX nor NC-CCS-II scaling curves

reach the minima within 1.655-1.911 μm, which sets these scaling curves apart from most other curves. The minimum point on APMEX scaling curve is within 1.911-2.207 μm, while that on NC-CCS-II is within 1.435-1.655 μm. For these two curves, particles within 1.655-1.911 μm no longer have the lowest scaling factors, thus the relative fractions of these particles increase significantly. **Figure 61a** and **Figure 61c** show that majority of aged sea salt and dust particles fall within the size range of 1.6 – 2.0 μm, thus these particles are impacted the most by a shift of scaling curve minimum. As a result, higher mass concentrations of aged sea salt and dust particles are obtained for the supermicron size range with the APMEX and NC-CCS-II scaling functions. One exception to this trend is that the scaling curve of NC-CCS-I does not reach the minimum between 1.655-1.911 μm, although its scaling results are similar to those with TexAQS, CIFEX, and Freeway scaling functions. The reason for this exception is not known; however, it shows that the change in scaling curve shape does not necessarily correspond to a change in the scaling results. One thing worth to point out is that all the reference APS scaling curves are only similar in shape, the actual scaling factor values vary substantially for the same particle diameter. Thus, it is expected that the absolute scaled mass concentrations would also vary considerably depending on the APS scaling function used. This difference in mass concentrations is also illustrated in **Figure 62** (a vs. b and c vs. d) where a different Y-axis scale is needed for the same study when using different scaling curves. Thus, comparing the absolute values of scaled particle type mass concentrations will not provide much insight on the true ambient concentrations.

d. APS Scaled Particle Mass Fraction

Although the mass concentrations obtained by scaling the test studies with APS scaling functions from reference studies do not reflect the real ambient concentrations, a remarkable consistency is observed in the mass fractions of individual particle types. The scaled major particle type mass fractions for the Fresno and Angiola studies are shown in **Figure 63**. Particles were segregated into submicron, supermicron and $PM_{2.5}$ size ranges for finer comparisons. Each pie chart corresponds to the mass fractions obtained with the scaling function from a specific reference study as listed on top. Besides the reference

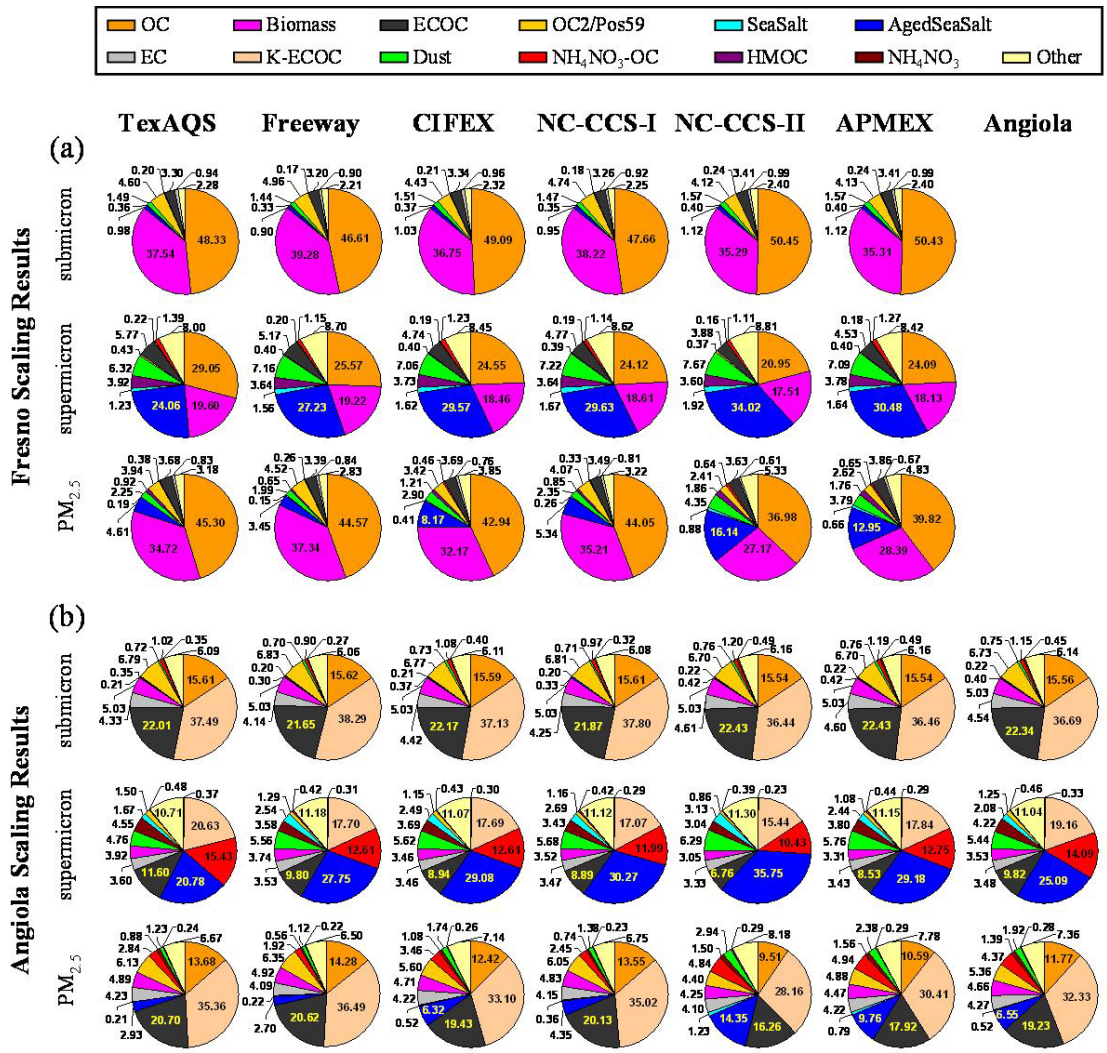

Figure 63: Fresno and Angiola individual particle type mass fractions for submicron, supermicron and PM2.5 range obtained with APS scaling functions from TexAQS, Freeway, CIFEX, NC-CCS, APMEX, and Angiola studies.

scaling functions, Angiola measurements are also scaled with co-located APS measurements for comparison purposes.

Surprising consistency can be observed in Figure 63 for the mass fractions of submicron particle types regardless of the scaling function used. In general, Fresno submicron particles consist 49% OC, 37% biomass, 4.5% Pos27, 3.3% ECOC, 1.5% dust, and 1.0% aged sea salt. The rest of the particle types account for less than 1% each in the mass fractions, and the unclassified particles account for 2.3% of total submicron mass. The standard deviations of each particle type mass fraction obtained with all 6 reference scaling functions are less than 9% of the average values, except for NH_4NO_3-OC which is 13%. Angiola scaled mass fractions are shown in **Figure 63b**. Scaled submicron particle type mass fractions also showed very good consistencies, with 16% OC, 37% K-ECOC, 22% ECOC, 6.8% Pos59, 5.0% biomass, 4.4% EC, and 1.1% NH_4NO_3-OC particle. Sea salt, aged sea salt, HMOC, NH_4NO_3, and dust account for less than 1% each, and the unclassified particles explain 6.1% of Angiola submicron mass. The mass fraction

standard deviations are less than 4% of the corresponding average values, with the exception of 12% for aged sea salt, 11% for NH_4NO_3-OC, and 22% for NH_4NO_3 particles. In addition to the consistency in submicron particle type mass fractions acquired with various APS scaling functions, **Figure 63b** also illustrates that similar results are obtained when scaling Angiola submicron particles with co-located APS scaling function and with reference study scaling functions. Therefore, a resonably accurate estimation of the mass fractions of submicron particle types can be acquired by scaling ATOFMS measurements with scaling functions from other studies.

Compared to the submicron scaling results, supermicron particles contain lower fractions of carbonaceous particles and higher fractions of aged sea salt, dust and NH_4NO_3 rich particles. More variation is obtained for the supermicron mass fractions obtained by using various scaling functions. One major factor causing this variation is the shift in scaling curve minima as discussed in section 6.4.4. The change in the minimum of the scaling curve at larger sizes can significantly increase the relative amount of the particles between 1.655-1.911 μm, into which most aged sea salt particles fall. This increase on aged sea salt mass fraction will then affect the mass fractions of other particle types. For Fresno particles in the supermicron size range, compared to utilizing other scaling functions, scaling with APMEX and NC-CCS-II leads to lower mass fractions of OC (22.5% instead of 25.8%), biomass (17.8% instead of 19.0%) and ECOC (4.2% instead of 5.1%) particles, and a higher fraction of aged sea salt particles (32.3% instead of 27.6%). Angiola scaled supermicron particle type mass fractions show similar patterns to those in Fresno. Moreover, the supermicron mass fractions obtained with co-located APS scaling function fall within the mass fraction range calculated with other scaling functions, showing that particle type mass fractions obtained with reference scaling functions are good estimates of the ambient aerosol concentrations.

The particle type mass concentrations for $PM_{2.5}$ is calculated by adding the mass concentrations of the corresponding types in the submicron and supermicron ranges. Although there appears to be more variations in the mass fractions, especially for the aged sea salt particles (varied from 3.4% to 16.1% in Fresno), it is mainly caused by the changes in the scaling curve minima, as mentioned earlier. **Figure 62** clearly illustrates the difference caused by scaling curves. Scaling Fresno and Angiola data with APMEX scaling function generates a second peak near 1.5 – 1.9 μm, in which most of the aged sea salt particles fall. This second peak is not present when scaling with the TexAQS scaling function. APMEX scaled mass concentrations contain a much higher fraction of the aged sea salt particles in the $PM_{2.5}$ range (13.0% for Fresno and 9.8% for Angiola) compared to those scaled with TexAQS (4.6% for Fresno and 2.9% for Angiola), causing the variations observed in the $PM_{2.5}$ mass fractions as shown in **Figure 63**.

iv. Conclusions

ATOFMS measurements at two ambient sampling locations, Fresno and Angiola in California's San Joaquin Valley, are scaled with APS scaling functions to obtain quantitative information on individual particle type mass fractions. The effect of APS scaling functions on the results was investigated by taking the scaling functions from five different studies acquired under a wide range of ambient conditions. The Angiola measurements were also scaled using co-located APS measurements to evaluate the results obtained from reference scaling functions.

Although the mass concentrations of individual particle types can vary more than one order of magnitude depending on the scaling functions used, nearly identical particle type mass fractions are observed in the submicron size range regardless of the APS scaling functions used. More variations in the mass fractions is observed for the supermicron and $PM_{2.5}$ size ranges, mainly caused by the shift on the scaling curve minimum point. Lower mass fractions of carbonaceous particles (44.5% instead of 49.9%) and higher fractions of aged sea salt (32.3% instead of 27.6%) and dust (7.4% instead of 6.9%) particles are obtained in Fresno when scaling with APMEX and NC-CCS-II scaling functions compared to using other scaling functions. Even though the mass fractions in the supermicron and $PM_{2.5}$ range are not as consistent as those in the submicron region when scaling with different APS scaling functions, we can still obtain the particle type mass fractions in these size ranges with errors less than 19%. Similar trends are observed in Angiola particle type mass fractions as those in Fresno. When Angiola measurements are scaled with a co-located APS scaling function, the submicron particle type mass fractions are almost identical to those obtained with reference scaling functions, the supermicron and $PM_{2.5}$ mass fractions also fall within the ranges obtained with reference scaling functions. Therefore, to obtain quantitative information from ATOFMS measurements from a study that does not have co-located APS measurements, the APS scaling functions from other studies can be used to provide a very good estimate of submicron particle type mass fractions and a close estimate of supermicron and $PM_{2.5}$ mass fractions.

v. Acknowledgements

This research was supported by the California Air Resources Board (Contract No. 04-336). The author would also like to thank John Holecek, Ryan Moffet, Laura Shields, Dr. David Sodeman, Matt Spencer and Steve Toner for providing the APS scaling functions for the reference studies.